Available online at www.sciencedirect.com
SCIENCE DIRECT®
Journal of Nuclear Materials 329–333 (2004) 1567–1570
journal of nuclear materials
www.elsevier.com/locate/jnucmat

Elastic–plastic FEM analysis on low cycle fatigue behavior for alumina dispersion-strengthened copper/stainless steel joint

H. Nishi *

Department of Nuclear Energy System, Japan Atomic Energy Research Institute (JAERI), 2-4 Shirakata-shirane, Tokai-mura, Ibaraki 319-1195, Japan

Abstract

Since the first wall and divertor components of fusion power plants are subjected to severe stresses caused by thermal expansion and electromagnetic forces, it is important to evaluate the fatigue strength of joints. In this study, elastic–plastic finite element analysis was performed for low cycle fatigue behavior of stainless steel/alumina dispersion-strengthened copper (DS Cu) joint in order to investigate the fatigue life and the fracture behavior of the joint. The results showed that a strain concentration occurred at the interface during low cycle fatigue, but as the strain range increased the strain concentration shifted away from the interface and into the DS Cu. The fatigue life and fracture location were evaluated taking into account of the strain concentration. Predictions of the fatigue life and fracture location were consistent with those measured by the low cycle fatigue test.

1. Introduction

Various aspects concerning interfacial cracking and fracture of dissimilar metal joints have been investigated in recent years [1–3]. Fracture along the interface between dissimilar metals is often encountered in engineering components such as the first wall and the divertor of fusion power plants. Alumina dispersion-strengthened copper (DS Cu) is a particularly attractive material for high temperature components because of its excellent thermal conductivity, strength retention and micro-structural stability at elevated temperatures. The DS Cu is therefore a good candidate material as a heat sink material for the first wall of an experimental fusion reactor. Since the first wall requires bonding of the DS Cu to austenitic stainless steel, we have carried out research exploring the strength of the joint between the DS Cu and 316 stainless steel [4–6].

It is important to evaluate the fatigue strength of the joint, since the first wall and the divertor components will be subjected to severe stresses caused by thermal expansion and electromagnetic forces. In the previous study [6], the low cycle fatigue test was performed for the joint between the DS Cu and 316 stainless steel, which was fabricated by a diffusion bonding at 1273 K for 1 h. The fatigue strength of the joint was smaller than that of the DS Cu, as shown Fig. 1. The joint fractured in the DS Cu near the interface for the case of small strain ranges. For high strain ranges, however, the fracture location shifted 6 mm away from the interface into the DS Cu. In this study, elastic–plastic finite element analysis was performed for the low cycle fatigue behavior of the joint in order to investigate the fatigue life and the fracture behavior of joint.

2. Procedure of FEM analysis

The FEM model was a parallel part of the round bar fatigue specimen, in which the DS Cu and stainless steel were bonded in the middle of parallel part, as indicated in Fig. 2(a). The mesh was divided among only a half of the specimen because of an axial symmetry of its deformation and was constructed with isoparametric

* Tel.: +81-29 282 5399/6489; fax: +81-29 282 5864/6489.
E-mail address: nishi@popsvr.tokai.jaeri.go.jp (H. Nishi).

0022-3115/$ - see front matter © 2004 Elsevier B.V. All rights reserved.
doi:10.1016/j.jnucmat.2004.04.169

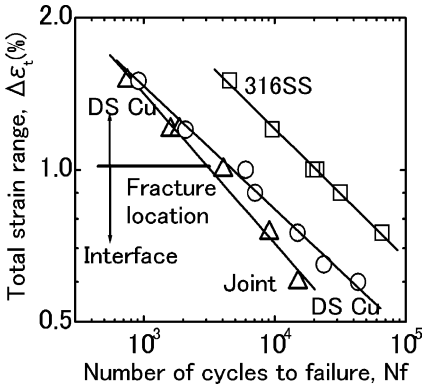

Fig. 1. Low cycle fatigue lives of joint, DS Cu and stainless steel.

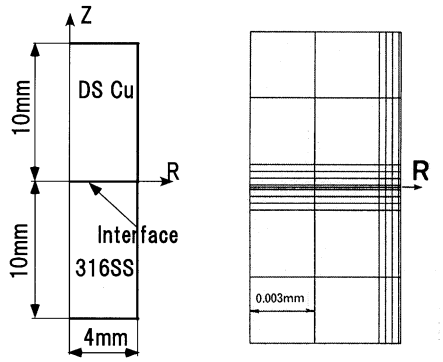

(a) half of specimen **(b)** mesh near edge

Fig. 2. FEM analysis model.

8-node biquadratic axisymmetric elements. The number of elements and nodes was 2450 and 9800 respectively. Taking into account of the stress singularity at the bonded edge, the element size was diminished as the element moved closer to the interface or the edge, as shown in Fig. 2(b). A ratio of the minimum element size to a radius of the specimen was 2.5×10^{-5}.

Young's moduli, Poisson's ratios and cyclic stress–strain curves of the stainless steel and DS Cu, which were obtained by tensile and low cycle fatigue test, are shown in Table 1 and Fig. 3 respectively. Comparing the cyclic stress–strain curves, the Young's modulus and strain hardening of the stainless steel was larger than those of the DS Cu. The stress–strain curve of stainless steel intersected that of DS Cu at strain amplitude of approximately 0.55%. In plastic range, the deformation stress of the stainless steel was smaller than that of DS Cu at less than the intersecting strain amplitude.

The elastic–plastic analysis was performed with a computer program ABAQUS on tensile and fatigue analysis. As for the boundary conditions, a uniform

Table 1
Used Young's moduli, Poisson's ratios

	DS Cu	316SS
E (GPa)	120	185
υ	0.34	0.3

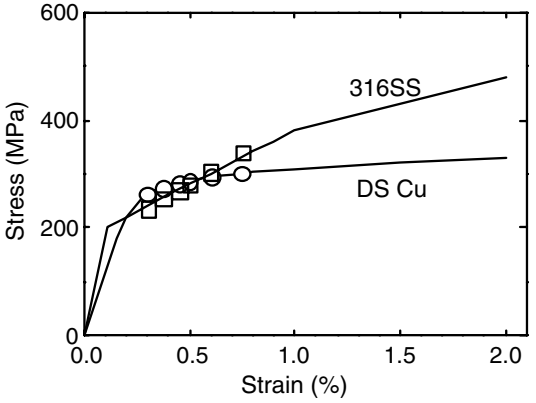

Fig. 3. Cyclic stress–strain curves used in analysis.

displacement was applied to the top nodes of model (DS Cu). The displacements of nodes on the z-axis and lower end (stainless steel) were fixed in the radial and z direction, respectively. With regard to the fatigue analysis, cyclic displacement was applied up to four cycles for total strain range $\Delta\varepsilon_t = 0.6\%$, 0.75%, 1.0%, 1.2%, 1.5% as a kinematic hardening material for DS Cu and stainless steel.

3. Results of analysis

3.1. Tensile analysis

Fig. 4 shows distributions of axial stress, σ_z, on the interface near the edge obtained by the tensile analysis. In this figure, the stress were compared with a ratio of distance from the edge, r, to the radius of the specimen, w, in respect of elastic and elastic–plastic analyses for nominal strain $\varepsilon = 0.2$–1.0%. Stress singularity existed slightly in the edge for the combination between stainless steel and DS Cu. According to Bogy's investigations for elastic problems [7,8], the singularity is expressed in order $r^{-\lambda}$ and the index λ is 0.0204 for this analyzed model. Fig. 4 designates the indexes λ, which are slopes of the stress distribution around the edge. In the case of the elastic analyses, the index λ is 0.0203 and is well in accordance with the theoretical result. As the strain was advanced to the plastic range $\varepsilon = 0.2$–0.5%, the stress singularity decreased, while the stress concentration occurred again near the edge at more than 0.75% nominal strain.

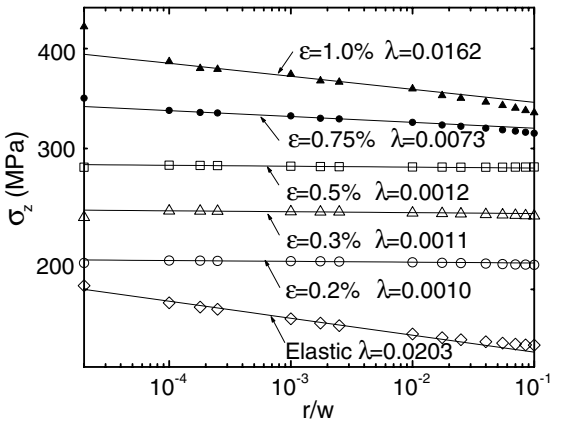

Fig. 4. Axial stress distribution on the interface near edge.

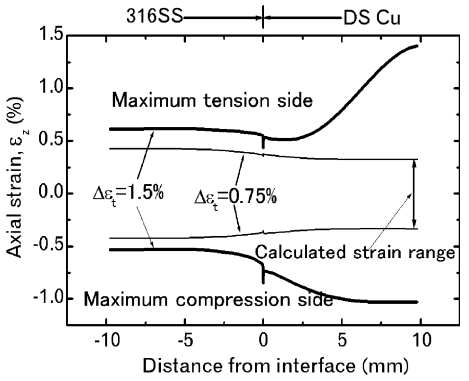

Fig. 5. Axial strain distribution of specimen surface along loading direction.

3.2. Fatigue analysis

As for the fatigue analysis, the results were discussed on the fourth cycle, because the stress–strain hysterysis loop was closed before the fourth cycle. Distributions of axial strain, ε_z, on specimen surface along the loading direction were designated in Fig. 5 as an example. In this figure, the strain distributions of the maximum tension and compression sides are shown for the strain range $\Delta\varepsilon_t = 0.75\%$ and 1.5%, for which the joint specimen fractured in the DS Cu near the interface and further into the DS Cu away from the interface in the fatigue test, respectively. At a strain range of $\Delta\varepsilon_t = 0.75\%$, the calculated strain range was lower in the DS Cu compared to that in the stainless steel owing to the fact that the cyclic stress–strain curve used for the FEM modeling shows that the stainless steel is slightly weaker than the DS Cu at this range. At $\Delta\varepsilon_t = 1.5\%$, however, the calculated strain range in the DS Cu is much higher than at the interface or in the stainless steel. These calculations support the experimental observation that at $\Delta\varepsilon_t = 0.75\%$ the failure occurred near the interface, but at higher strain range the failure location shifted away from the interface and further into the DS Cu.

In order to discuss the fracture location and fatigue life of the low cycle fatigue test, the calculated strain range on the end of DS Cu, the interface (DS Cu 0.01 mm from interface) and the end of stainless steel were compared for the various strain ranges, as shown in Table 2. Table 2 also designated the observed number of cycles to failure, the fracture location and the predicted

Table 2
Results of calculated strain range and comparison between predicted and observed N_f

$\Delta\varepsilon_t$ (%)	Position	Calculated $\Delta\varepsilon$ (%)	Predicted N_f	Observed N_f fracture location
0.6	DS Cu	0.554	54 600	15 100
	Interface (DS Cu)	0.602	○ 38 000	Interface
	Stainless steel	0.65	112 000	
0.75	DS Cu	0.657	27100	9080
	Interface (DS Cu)	0.753	○ 15 400	Interface
	Stainless steel	0.846	40 000	
1	DS Cu	0.896	7560	4056
	Interface (DS Cu)	1.03	○ 4250	Interface
	Stainless steel	1.09	14 900	
1.2	DS Cu	1.33	○ 1490	1590
	Interface (DS Cu)	1.22	2120	DS Cu
	Stainless steel	1.14	12 500	
1.5	DS Cu	2.43	○ 140	750
	Interface (DS Cu)	1.28	1750	DS Cu
	Stainless steel	1.15	12 000	

number of cycles to failure, which were obtained from substituting the calculated strain range, $\Delta\varepsilon$, for each low cycle fatigue life obtained by the fatigue test in respect of DS Cu and stainless steel base metals. The minimum predicted number of cycles to failure among the parts of the DS Cu, interface and stainless steel was marked with a circle. As can be seen, the predicted fatigue life and the fracture location were consistent with the low cycle fatigue test. The fracture location in the specimen depending on its strain range was attributed to the strain concentration.

4. Conclusions

1. An elastic stress singularity existed slightly at the interface between the stainless steel and DS Cu. As the strain was increased to the plastic range, the stress singularity decreased, while the stress concentration occurred again near the interface at larger strain.
2. The fracture location in the specimen depending on its strain range was attributed to its strain concentration.
3. The predicted fatigue life and the fracture location were consistent with the low cycle fatigue test. The low cycle fatigue life of joint can be understood from the low cycle fatigue life of base metals using FEM analysis.

References

[1] C.F. Shih, R.J. Asaro, J. Appl. Mech. 56 (1989) 763.
[2] R. Yuuki, S.B. Cho, Eng. Fract. Mech. 34 (1989) 179.
[3] S. Aoki, K. Kishimoto, N. Takeuchi, Int. J. Fract. 55 (1992) 363.
[4] H. Nishi, Y. Muto, K. Sato, J. Nucl. Mater. 212–215 (1994) 1585.
[5] H. Nishi, K. Kikuchi, J. Nucl. Mater. 258–263 (1998) 281.
[6] H. Nishi, T. Araki, J. Nucl. Mater. 283–287 (2000) 1234.
[7] D.B. Bogy, Int. J. Solids Struct. 6 (1970) 1287.
[8] D.B. Bogy, J. Appl. Mech. 38 (1971) 377.